Supplementary information

1. Theoretical

1.1 Mass transfer and Nanobody exchange kinetics model

The microfluidic chromatographic column was modelled as a homogeneous packed bed of length l $[\mathrm{m}]$ of porous agarose particles with a diameter d_p $[\mathrm{m}]$. Flow and concentration gradients of solutes were only considered in the axial direction x and boundary effects from the channel side walls were not taken into account. For a solute with bulk concentration C, mass transfer and Nanobody exchange kinetics in the column can be modelled as [1]:

$$\frac{\partial C}{\partial x} = D_\mathrm{ax}\frac{\partial^2 C}{\partial^2 x} - u\frac{\partial C}{\partial x} + R_\mathrm{exch} \tag{1}$$

Here, D_ax is the axial dispersion coefficient $\left[\frac{\mathrm{m}^2}{\mathrm{s}}\right]$ and u is the pore velocity $\left[\frac{\mathrm{m}}{\mathrm{s}}\right]$, that can be calculated as [2]:

$$u = \frac{u_\mathrm{s}}{\varepsilon} \tag{2}$$

wherein u_s is the superficial velocity = $\frac{Q}{Ar}$, with Q the flow rate $\left[\frac{\mathrm{m}^3}{\mathrm{s}}\right]$ and Ar the cross-sectional area of the column $\left[\mathrm{m}^2\right]$. The external porosity ε (outside of particles), was assumed to be uniform and is $\varepsilon = 0.4$ for randomly packed particles [3]. The Nanobody exchange reaction term R_exch, made explicit in section 1.3, describes the association of analyte A to trapper T to form an analyte-trapper complex AT, or the dissociation of the complex, or the association of A to stripper S to form an analyte-stripper complex AS. Due to its high affinity, we assumed stripper binds the analyte irreversibly. The association and dissociation kinetics were described with Langmuir kinetics [1], where k_on $\left[\mathrm{M^{-1}s^{-1}}\right]$ and k_off $\left[\mathrm{s^{-1}}\right]$ are the association and dissociation constants.

To include the effect of mass transfer of solutes from the bulk solution to a stationary sublayer in and around the particles, we worked with a lumped mass transfer coefficient k_m $\left[\frac{\mathrm{L}}{\mathrm{m^2 s}}\right]$. For simplicity, the analyte, stripper and analyte-stripper complex were assumed to have the same axial dispersion coefficient, molecular diffusion coefficient outside the particles D_mol $\left[\frac{\mathrm{m}^2}{\mathrm{s}}\right]$ and molecular diffusion coefficient inside the particles D_part $\left[\frac{\mathrm{m}^2}{\mathrm{s}}\right]$. The particle Sherwood number was found in literature to be $\mathrm{Sh_p} = 10$ [4], while the bed Sherwood number Sh was calculated by extrapolating [5]:

$$\mathrm{Sh} = \frac{13}{1+2.1\nu_\mathrm{i}} + 8.6\nu_\mathrm{i}^{0.21} \tag{3}$$

Here, ν_i is the reduced interstitial velocity = $\frac{\varepsilon_\mathrm{T}}{\varepsilon}\frac{u_\mathrm{s} d_\mathrm{p}}{D_\mathrm{mol}}$, with ϵ_T the total porosity $= \varepsilon + (1-\varepsilon)\varepsilon_\mathrm{p}$ where ε_p is the particle porosity, which is $\varepsilon_\mathrm{p} = 0.79$ for agarose [6]. The lumped mass transfer coefficient k_m is then defined as [4,7]:

$$\frac{1}{k_\mathrm{m}} = \frac{1}{k_\mathrm{e}} + \frac{1}{k_\mathrm{p}} \tag{4}$$

$$k_\mathrm{e} = \mathrm{Sh}\frac{D_\mathrm{mol}}{d_\mathrm{p}}10^3 \tag{5}$$

$$k_\mathrm{p} = \mathrm{Sh_p}\frac{D_\mathrm{part}}{d_\mathrm{p}}10^3 \tag{6}$$

1.2 Axial dispersion in an empty capillary and in a column

If a solute is injected into an empty capillary or a column, the pulse spreads due to different effects, such as the parabolic velocity profile of pressure-driven flow [8], eddy diffusion, longitudinal molecular diffusion and diffusion into and out of porous particles (resistance to mass transfer) [9]. Additionally, variations in the velocity profile caused by capillary-bed transitions or non-cylindrical columns, where the packing is less dense near the walls, can lead to pulse broadening. These broadening effects are together called axial (or longitudinal) dispersion. For a pulse injection of solute, these effects can be described by the dimensionless distribution of residence times $E(\theta)$ as follows [10,11]:

$$E(\theta) = \sqrt{\frac{\mathrm{Pe}}{4\pi\theta}} \exp\left(\frac{-\mathrm{Pe}(1-\theta)^2}{4\theta}\right) \tag{7}$$

Here, θ is the dimensionless residence time $\frac{t}{\bar{t}}$, where $\bar{t}$ is the mean residence time $\frac{V}{Q}$ [s], with V the capillary or chip void volume + half the injected volume. The Peclet number Pe is $\frac{lu}{D_{\mathrm{ax}}}$ for a capillary, where l is the capillary length [m] and u is the velocity $\frac{Q}{Ar}\left[\frac{\mathrm{m}}{\mathrm{s}}\right]$, with Ar the cross-sectional area of the capillary $[\mathrm{m}^2]$. Pe is $\frac{d_{\mathrm{p}}u}{D_{\mathrm{ax}}}$ for a column, where u is the pore velocity. Equation 7 can be used for a finite column if $\frac{lu}{D_{\mathrm{ax}}} \geq 10$ [10].

For an injection concentration C_0 [M] into an initially empty capillary that is sufficiently long (semi-infinite), the tracer concentration at the end of the capillary is [11,12]:

$$C = \frac{C_0}{2}\left(\mathrm{erfc}\left(\frac{l-ut}{\sqrt{4D_{\mathrm{ax}}t}}\right) + \exp\left(\frac{lu}{D_{\mathrm{ax}}}\right)\mathrm{erfc}\left(\frac{l+ut}{\sqrt{4D_{\mathrm{ax}}t}}\right)\right) \tag{8}$$

Where $\mathrm{erfc}(x) = 1 - \mathrm{erf}(x)$, with $\mathrm{erf}(x) = \frac{2}{\sqrt{\pi}}\int_0^x \exp(-t^2)dt$.

1.3 Model equations for trapping and stripping

A distinction was made between the concentration of free solutes in bulk $[solute]$ and in the sublayer $[solute_{\mathrm{s}}]$. These are volume concentrations $\left[\mathrm{M} = \frac{\mathrm{mol}}{\mathrm{L}}\right]$, while the concentration of solutes immobilised on the particles is indicated as $[solute]^*$ and this is a surface concentration $\left[\frac{\mathrm{mol}}{\mathrm{m}^2}\right]$. Then $[solute] = [solute]^* a$, with a the specific particle surface area, i.e. the area per volume liquid $\left[\frac{\mathrm{m}^2}{\mathrm{L}}\right]$. A calculation of a for a column of porous particles is made in Supplementary materials 1.6. $[\mathrm{T}]_0^*$ is the concentration of trapper coated on the particles:

$$[\mathrm{T}]_0^* = \frac{1}{N_{\mathrm{A}}}\frac{1}{\alpha 10^{-18}} \tag{9}$$

Here, $N_{\mathrm{A}} = 6.02\ 10^{23}$ is the Avogadro number $[\mathrm{mol}^{-1}]$ and α is the surface for one trapper $[\mathrm{nm}^2]$. We assume $[\mathrm{T}]_0^*$ is low enough so bound analyte does not overlap with unbound sites, which is required to use Langmuir reaction kinetics. Since solutes in the stationary sublayer or immobilised on the particles do not move, the first two terms in Equation 1 become zero.

The model is split into a trapping and a stripping phase. During the trapping phase, the target analyte is injected and unbound material is washed out. During the stripping phase, stripper is injected and the stripped material is eluted by extra flow. Following governing Equation 1, the model consists of following equations:

Trapping:

$$\frac{\delta[\mathrm{A}]}{\delta t} = D_{\mathrm{ax}}\frac{\delta^2[\mathrm{A}]}{\delta x^2} - u\frac{\delta[\mathrm{A}]}{\delta x} - ak_{\mathrm{m}}([\mathrm{A}] - [\mathrm{A_s}]) \quad (10)$$

$$\frac{\delta[\mathrm{A_s}]}{\delta t} = ak_{\mathrm{m}}([\mathrm{A}] - [\mathrm{A_s}]) - k_{\mathrm{on,T}}[\mathrm{A_s}][\mathrm{T}]^* a + k_{\mathrm{off,T}}[\mathrm{AT}]^* a \quad (11)$$

$$\frac{\delta[\mathrm{AT}]^*}{\delta t} = k_{\mathrm{on,T}}[\mathrm{A_s}][\mathrm{T}]^* - k_{\mathrm{off,T}}[\mathrm{AT}]^* \quad (12)$$

$$[\mathrm{T}]_0^* = [\mathrm{AT}]^* + [\mathrm{T}]^* \quad (13)$$

Stripping:

$$\frac{\delta[\mathrm{S}]}{\delta t} = D_{\mathrm{ax}}\frac{\delta^2[\mathrm{S}]}{\delta x^2} - u\frac{\delta[\mathrm{S}]}{\delta x} - ak_{\mathrm{m}}([\mathrm{S}] - [\mathrm{S_s}]) - k_{\mathrm{on,S}}[\mathrm{A}][\mathrm{S}] \quad (14)$$

$$\frac{\delta[\mathrm{A}]}{\delta t} = D_{\mathrm{ax}}\frac{\delta^2[\mathrm{A}]}{\delta x^2} - u\frac{\delta[\mathrm{A}]}{\delta x} - ak_{\mathrm{m}}([\mathrm{A}] - [\mathrm{A_s}]) - k_{\mathrm{on,S}}[\mathrm{A}][\mathrm{S}] \quad (15)$$

$$\frac{\delta[\mathrm{AS}]}{\delta t} = D_{\mathrm{ax}}\frac{\delta^2[\mathrm{AS}]}{\delta x^2} - u\frac{\delta[\mathrm{AS}]}{\delta x} - ak_{\mathrm{m}}([\mathrm{AS}] - [\mathrm{AS_s}]) + k_{\mathrm{on,S}}[\mathrm{A}][\mathrm{S}] \quad (16)$$

$$\frac{\delta[\mathrm{S_s}]}{\delta t} = ak_{\mathrm{m}}([\mathrm{S}] - [\mathrm{S_s}]) - k_{\mathrm{on,S}}[\mathrm{A_s}][\mathrm{S_s}] \quad (17)$$

$$\frac{\delta[\mathrm{A_s}]}{\delta t} = ak_{\mathrm{m}}([\mathrm{A}] - [\mathrm{A_s}]) + k_{\mathrm{off,T}}[\mathrm{AT}]^* a - k_{\mathrm{on,T}}[\mathrm{A_s}][\mathrm{T}]^* a - k_{\mathrm{on,S}}[\mathrm{A_s}][\mathrm{S_s}] \quad (18)$$

$$\frac{\delta[\mathrm{AS_s}]}{\delta t} = ak_{\mathrm{m}}([\mathrm{AS}] - [\mathrm{AS_s}]) + k_{\mathrm{on,S}}[\mathrm{A_s}][\mathrm{S_s}] \quad (19)$$

$$\frac{\delta[\mathrm{AT}]^*}{\delta t} = k_{\mathrm{on,T}}[\mathrm{A_s}][\mathrm{T}]^* - k_{\mathrm{off,T}}[\mathrm{AT}]^* \quad (20)$$

$$[\mathrm{T}]_0^* = [\mathrm{AT}]^* + [\mathrm{T}]^* \quad (21)$$

1.4 Initial conditions model

Trapping:

at $t = 0$:

$$[\mathrm{A}] = 0 \quad (22)$$

$$[\mathrm{A_s}] = 0 \quad (23)$$

$$[\mathrm{AT}]^* = 0 \quad (24)$$

Stripping:

at $t = 0$:

$$[\mathrm{S}] = 0 \quad (25)$$

$$[\mathrm{A}] = [\mathrm{A}]_{\text{end trapping}} = [\mathrm{A}]_0 \quad (26)$$

$$[\mathrm{AS}] = 0 \quad (27)$$

$$[\mathrm{S_s}] = 0 \quad (28)$$

$$[\mathrm{A_s}] = [\mathrm{A_s}]_{\text{end trapping}} = [\mathrm{A_s}]_0 \quad (29)$$

$$[\mathrm{AS_s}] = 0 \quad (30)$$

$$[\mathrm{AT}]^* = [\mathrm{AT}]^*_{\text{end trapping}} = [\mathrm{AT}]_0^* \quad (31)$$

1.5 Boundary conditions model

Trapping:

at $x = 0$:

$$[\mathrm{A}] = [\mathrm{A}]_0 \qquad \text{for } 0 < t \leq t_{\mathrm{trapping}} \tag{32}$$

$[A]_0$ is the injection concentration of analyte

$$[A] = 0 \qquad \text{for } t_{\mathrm{trapping}} < t \leq t_{\mathrm{trapping}} + t_{\mathrm{wash}} \tag{33}$$

t_{trapping} is the trapping run time, t_{wash} is the wash run time

$$\frac{\delta[\mathrm{A_s}]}{\delta x} = 0 \tag{34}$$

$$\frac{\delta[\mathrm{AT}]^*}{\delta x} = 0 \tag{35}$$

at $x = l$:

$$\frac{\delta[\mathrm{A}]}{\delta x} = 0 \tag{36}$$

$$\frac{\delta[\mathrm{A_s}]}{\delta x} = 0 \tag{37}$$

$$\frac{\delta[\mathrm{AT}]^*}{\delta x} = 0 \tag{38}$$

Stripping:

at $x = 0$:

$$[\mathrm{S}] = [\mathrm{S}]_0 \qquad \text{for } 0 < t \leq t_{\mathrm{stripping}} \tag{39}$$

$[\mathrm{S}]_0$ is the injection concentration of stripper

$$[\mathrm{S}] = 0 \qquad \text{for } t_{\mathrm{stripping}} < t \leq t_{\mathrm{stripping}} + t_{\mathrm{extra}} \tag{40}$$

$t_{\mathrm{stripping}}$ is the stripping run time, t_{extra} is the extra flow run time

$$[\mathrm{A}] = 0 \tag{41}$$

$$[\mathrm{AS}] = 0 \tag{42}$$

$$\frac{\delta[\mathrm{S_s}]}{\delta x} = 0 \tag{43}$$

$$\frac{\delta[\mathrm{A_s}]}{\delta x} = 0 \tag{44}$$

$$\frac{\delta[\mathrm{AS_s}]}{\delta x} = 0 \tag{45}$$

$$\frac{\delta[\mathrm{AT}]^*}{\delta x} = 0 \tag{46}$$

at $x = l$:

$$\frac{\delta[\mathrm{S}]}{\delta x} = 0 \tag{47}$$

$$\frac{\delta[\mathrm{A}]}{\delta x} = 0 \tag{48}$$

$$\frac{\delta[\mathrm{AS}]}{\delta x} = 0 \tag{49}$$

$$\frac{\delta[\mathrm{S_s}]}{\delta x} = 0 \tag{50}$$

$$\frac{\delta[\mathrm{A_s}]}{\delta x} = 0 \tag{51}$$

$$\frac{\delta[\mathrm{AS_s}]}{\delta x} = 0 \tag{52}$$

$$\frac{\delta[\mathrm{AT}]^*}{\delta x} = 0 \tag{53}$$

For injections equal to or bigger than 10 µL, these boundary conditions are corrected for axial dispersion of the injection plugs in the capillary in front of the column. Following Equation 8, Equation 32 is replaced by:

$$[\mathrm{A}] = \frac{[\mathrm{A}]_0}{2}\left(\operatorname{erfc}\left(\frac{l-ut}{\sqrt{4D_{\mathrm{ax}}t}}\right) + \exp\left(\frac{lu}{D_{\mathrm{ax}}}\right)\operatorname{erfc}\left(\frac{l+ut}{\sqrt{4D_{\mathrm{ax}}t}}\right)\right) \tag{54}$$

and Equation 39 is replaced by:

$$[\mathrm{S}] = \frac{[\mathrm{S}]_0}{2}\left(\operatorname{erfc}\left(\frac{l-ut}{\sqrt{4D_{\mathrm{ax}}t}}\right) + \exp\left(\frac{lu}{D_{\mathrm{ax}}}\right)\operatorname{erfc}\left(\frac{l+ut}{\sqrt{4D_{\mathrm{ax}}t}}\right)\right) \tag{55}$$

Similarly, Equation 33 is replaced by:

$$[\mathrm{A}] = [\mathrm{A}]_0 - \frac{[\mathrm{A}]_0}{2}\left(\operatorname{erfc}\left(\frac{l-ut}{\sqrt{4D_{\mathrm{ax}}t}}\right) + \exp\left(\frac{lu}{D_{\mathrm{ax}}}\right)\operatorname{erfc}\left(\frac{l+ut}{\sqrt{4D_{\mathrm{ax}}t}}\right)\right) \tag{56}$$

and Equation 40 is replaced by:

$$[\mathrm{S}] = [\mathrm{S}]_0 - \frac{[\mathrm{S}]_0}{2}\left(\operatorname{erfc}\left(\frac{l-ut}{\sqrt{4D_{\mathrm{ax}}t}}\right) + \exp\left(\frac{lu}{D_{\mathrm{ax}}}\right)\operatorname{erfc}\left(\frac{l+ut}{\sqrt{4D_{\mathrm{ax}}t}}\right)\right) \tag{57}$$

These boundary conditions are only valid if $[\mathrm{A}]_0$ or $[\mathrm{S}]_0$ are reached at the beginning of the column within the trapping or stripping time respectively.

1.6 Calculation of the specific particle surface area

The network of agarose filaments in the porous particles is represented as a cubic grid consisting of equal cylinders, where the distance between parallel cylinders is the pore size [13].

$$\begin{aligned}\frac{N_{\mathrm{cylinders}}}{V_{\mathrm{column}}} &= \frac{3V_{\mathrm{agarose}}}{(d+d_{\mathrm{filament}})^3 V_{\mathrm{column}}} \\ &= \frac{3(1-\epsilon)}{(d+d_{\mathrm{filament}})^3} \\ &= 3.76\,10^{21}\ [\mathrm{cylinders/m^3}]\end{aligned} \tag{58}$$

d is pore size of 6% agarose = 70 nm [14]

d_{filament} is agarose filament diameter = 8.2 nm [15]

$$\begin{aligned}a &= \frac{\mathrm{area}}{V_{\mathrm{liquid}}} \\ &= \frac{1}{\varepsilon}\frac{N_{\mathrm{cylinders}}}{V_{\mathrm{column}}} * \mathrm{area}_{\mathrm{cylinder}} \\ &= \frac{1}{\varepsilon}\frac{N_{\mathrm{cylinders}}}{V_{\mathrm{column}}} * \pi * d_{\mathrm{filament}} * d \\ &= \frac{1}{\varepsilon} 3.76\,10^{21} * \pi * 8.2\,10^{-9} * 70\,10^{-9} \\ &= \frac{6.8\,10^3}{\varepsilon}\left[\frac{\mathrm{m^2}}{\mathrm{L}}\right]\end{aligned} \tag{59}$$

The presence of 200 nm magnetite cores in the particles is neglected here.

2. Scanning electron microscope images chip

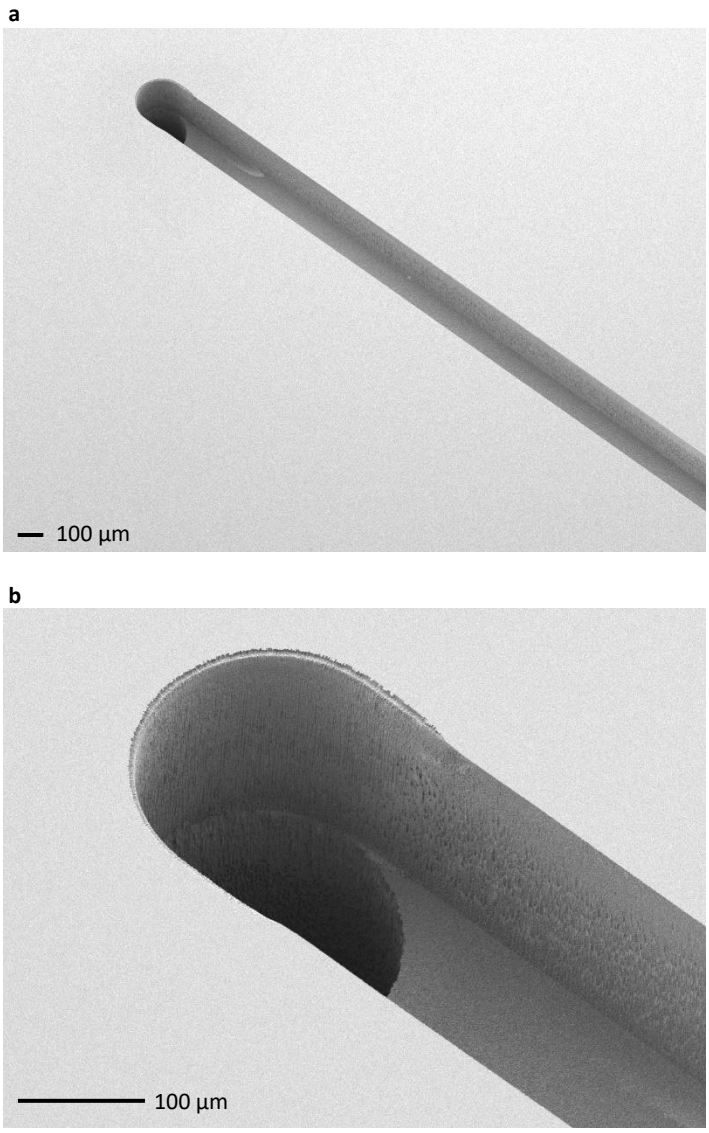

Fig. 1*: Scanning electron microscope images of part of the chip channel. (a) Magnification x43. (b) Zoomed in on the hole at the end of the channel, magnification x230. Images were acquired with a JSM 7610FPlus FEG from JEOL.*

3. Static GFP-binding capacity of Nb61-particles

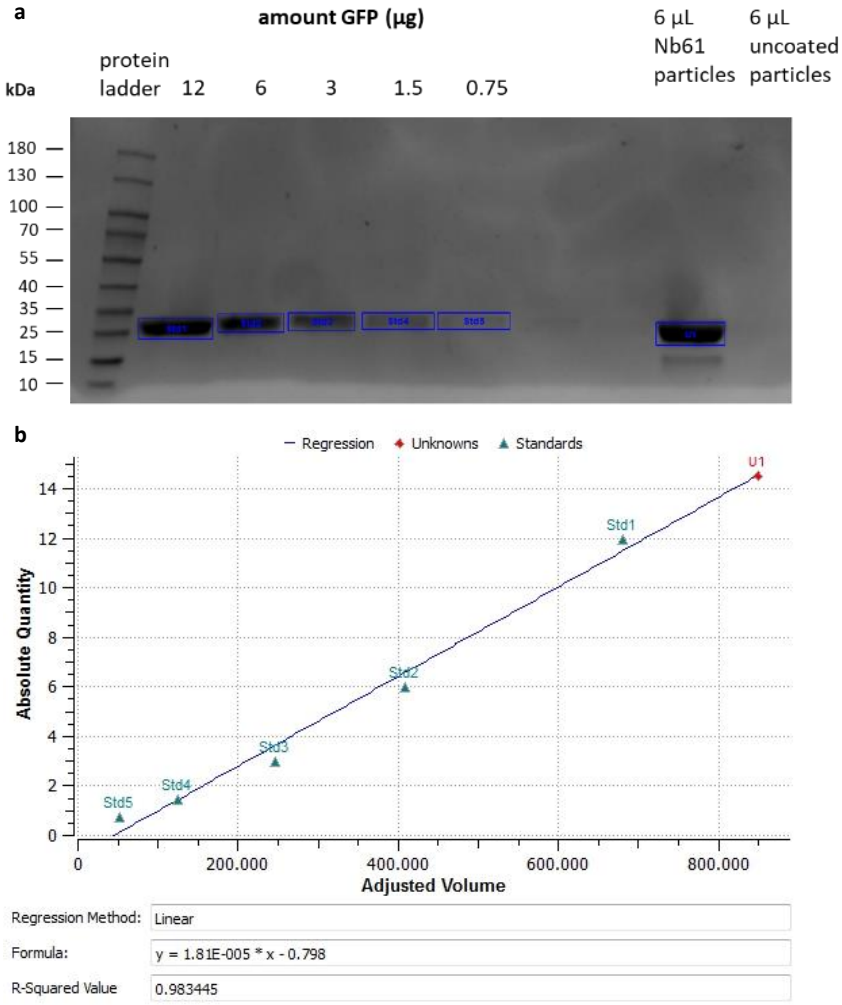

***Fig. 2**: Static GFP-binding capacity Nb61-particles. (a) Nb61-coated and uncoated PureCube particles were incubated for 1 h with GFP-specific Nb61, boiled and loaded on an SDS-PAGE gel next to a protein ladder and different GFP amounts. (b) Employing a standard curve made with the volume tool of Bio-Rad, the GFP-binding capacity was estimated to be 14.4 µg (U1)/6 µL = 2.4 µg/µL.*

4. Standard curve

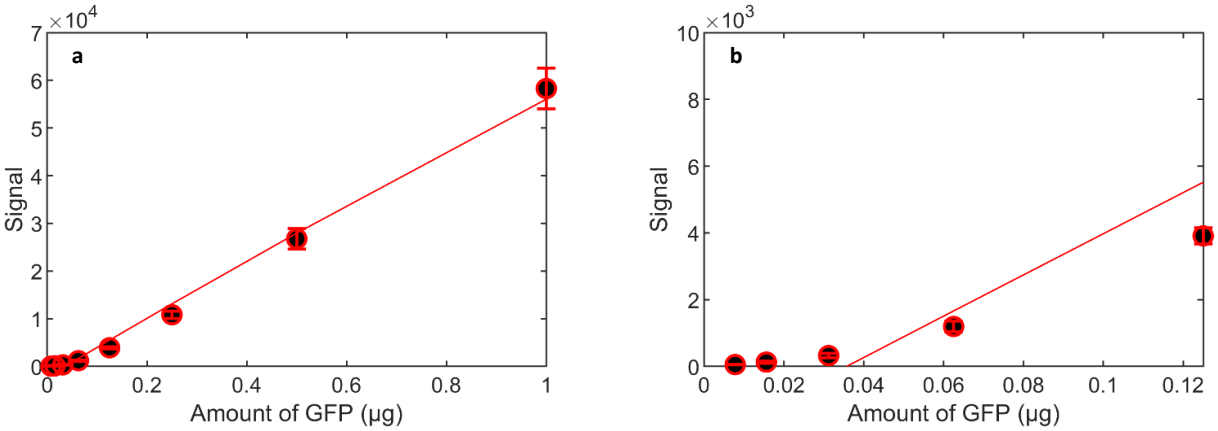

***Fig. 3**: Standard curve for GFP peaks measured with a fluorescence detector. (a) The standard curve was fitted with an R^2 of 0.9981 to be -4.17 10^3 x^2 + 6.24 10^4 x -2.22 10^3. (b) Zoomed in on lower amounts of GFP.*

5. Axial dispersion in empty capillary and in column

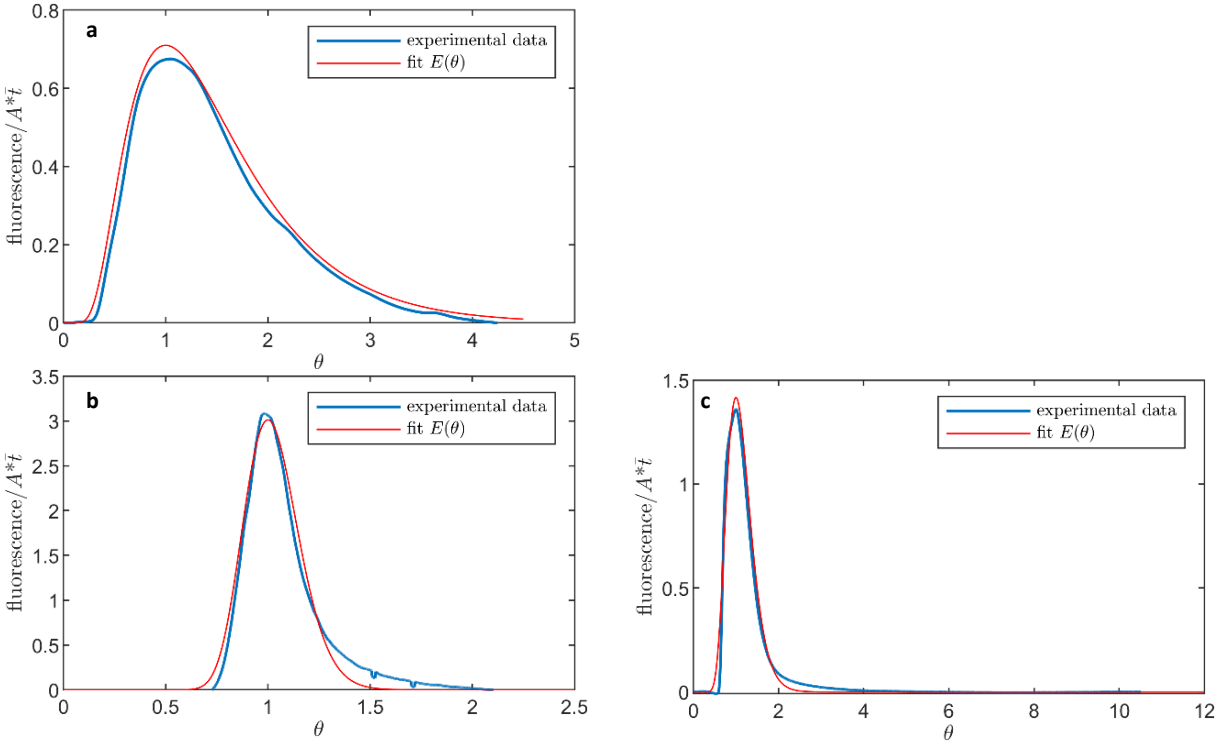

***Fig. 4**: Axial dispersion in an empty capillary and in a column. The distribution of residence times E of an injected solute fitted through normalised experimental fluorescence peaks in (a) an empty capillary: R^2 = 0.9842, (b) a column at 1 µL/min: R^2 = 0.9805 and (c) a column at 10 µL/min: R^2 = 0.9821.*

***Table 1**: Axial dispersion coefficient in an empty capillary and column at different flow rates, determined by fitting the distribution of residence times of an injected solute through normalised experimental fluorescence peaks. The axial dispersion coefficients in an empty capillary at different flow rates were calculated proportionally.*

	$D_{ax}\left[\frac{m^2}{s}\right]$	95% confidence bounds
Empty capillary with Q = 10 µL/min	2.986 10^{-3}	2.960 10^{-3}, 3.012 10^{-3}
Column with Q = 1 µL/min	1.676 10^{-7}	1.669 10^{-7}, 1.683 10^{-7}
Column with Q = 10 µL/min	7.581 10^{-6}	7.537 10^{-6}, 7.625 10^{-6}
Column with Q = 20 µL/min (linear extrapolation)	1.582 10^{-5}	

6. Nanobody exchange reaction kinetics

***Table 2**: Nanobody exchange reaction kinetic parameters of Nb207 and its double and triple mutants Nb16 and Nb61 determined via biolayer interferometry in an Octet R8 (Sartorius).*

	k_{off} x 10^{-4} (s^{-1})	Standard error x 10^{-4}	k_{on} x 10^5 (M^{-1} s^{-1})	Standard error x 10^5	K_D (nM) k_{off}/k_{on}	Half-life $\ln(2)/k_{off}$ (s)
Nb207	0.077 (average of 3 highest concentrations)	0.022	5.1 (average of 4 lowest concentrations)	0.51	0.015	90 000
Nb16	20 (average of 3 middle concentrations)	1.7	2.6 (average of 3 middle concentrations)	1.0	7.8	350
Nb61	1300 (average of 3 highest concentrations)	24	2.8 (average of 3 highest concentrations)	1.1	440	5

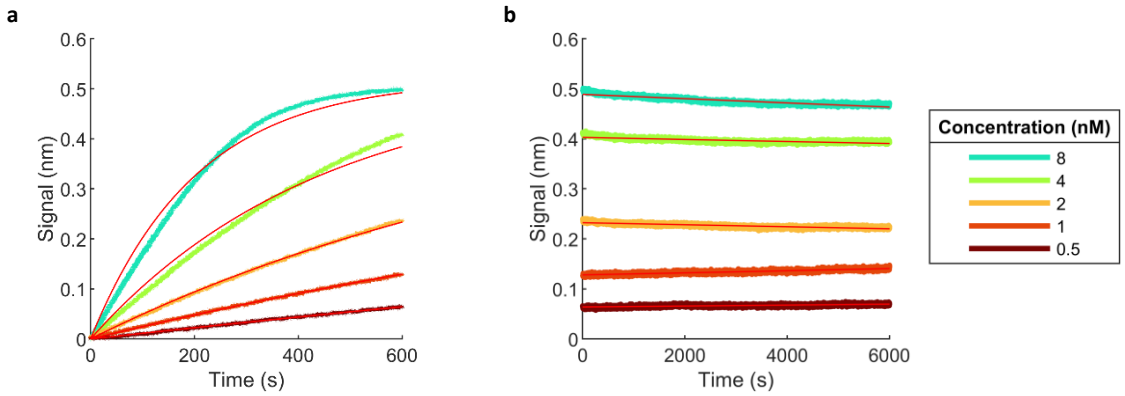

***Fig. 5**: Octet characterisation of GFP binder Nb207. (a) association curves of Nb207, (b) dissociation curves of Nb207. Data analysis was done in MATLAB, first smoothing the data, subtracting a reference curve (sensor incubated with buffer instead of Nb207) and aligning all curves at the start of association. Red lines show a one phase decay model fitted through the dissociation curve [16] and an association kinetics model fitted through the association curve [17]. R^2 is 0.9845, 0.9871, 0.9989, 0.9981, 0.9938 in a, 0.8505, 0.6102, 0.7277, 0.8127, 0.5042 in b.*

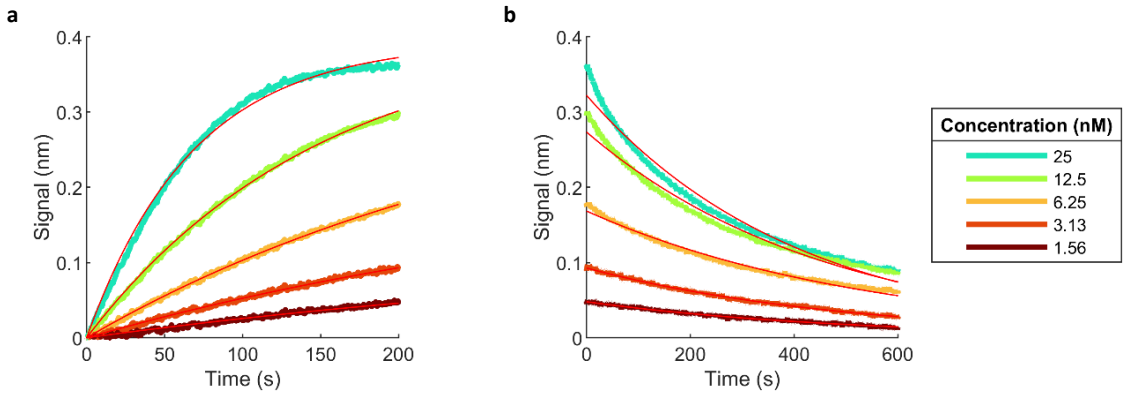

***Fig. 6**: Octet characterisation of GFP binder Nb16. (a) association curves of Nb16, (b) dissociation curves of Nb61. Data analysis was done in MATLAB, first smoothing the data, subtracting a reference curve (sensor incubated with buffer instead of Nb16) and aligning all curves at the start of association. Red lines show a one phase decay model fitted through the dissociation curve [16] and an association kinetics model fitted through the association curve [17]. R^2 is 0.9952, 0.9990, 0.9990, 0.9958, 0.9805 in a, 0.9780, 0.9809, 0.9878, 0.9904, 0.9741 in b.*

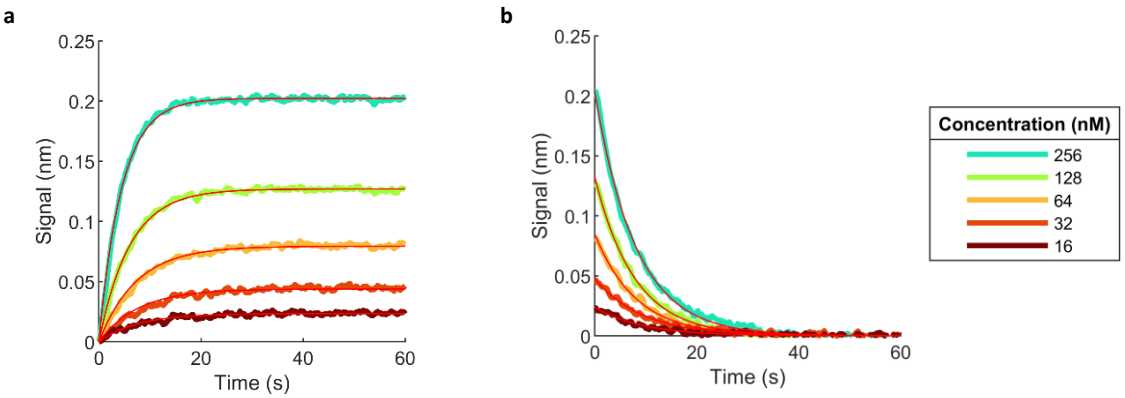

***Fig. 7**: Octet characterisation of GFP binder Nb61. (a) association curves of Nb61, (b) dissociation curves of Nb61. Data analysis was done in MATLAB, first smoothing the data, subtracting a reference curve (sensor incubated with buffer instead of Nb61) and aligning all curves at the start of association. Red lines show a one phase decay model fitted through the dissociation curve [16] and an association kinetics model fitted through the association curve [17]. R^2 is 0.9967, 0.9962, 0.9905, 0.9644, 0.9345 in a, 0.9972, 0.9925, 0.9853, 0.9832, 0.9458 in b.*

7. Variation of the injection profile of the autosampler

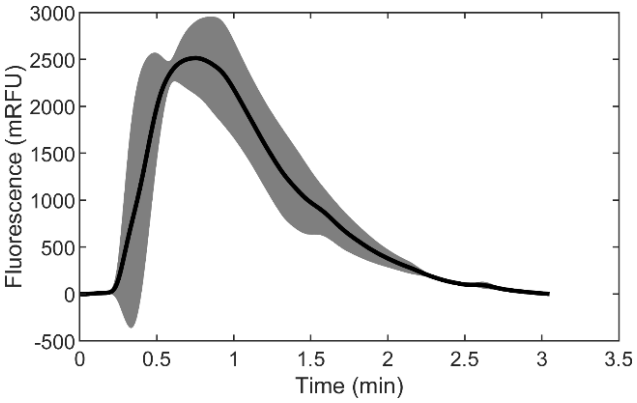

***Fig. 8**: Variation of injection profile autosampler. Triplicates of 10 µL 0.5 µg GFP injected in an empty capillary at 10 µL/min. Plotted using MATLABs function stdshade [18].*

8. Mass spectrometry

***Table 3**: List of all proteins identified via LC-MS in the elution of a µNANEX purification of 20 µL yeast lysate expressing PGI1-GFP. Data analysis was performed by means of PEAKS studio 7.5 (Bioinformatics Solutions). De novo sequencing and database searches (Swiss-Prot database, downloaded on 17/07/2024) were performed with a 10 ppm precursor mass tolerance and 0.02 Da fragment tolerance. Iodoacetamide alkylation of Cysteine was set as a fixed modification while the oxidation of Methionine and N-terminal acetylation were set as variable. The False Discovery Rate on the peptide level was set to 0.1%. Only proteins with more than one identified peptide were included in the list.*

Protein code	-10lgP	#Peptides	#Unique	Post-translational modifications	Description
P00925|ENO2_YEAST	351.52	16	8	Phenethyl isothiocyanate	Enolase 2 OS=Saccharomyces cerevisiae (strain ATCC 204508 / S288c) OX=559292 GN=ENO2 PE=1 SV=2
P00560|PGK_YEAST	316.08	24	23	Acetylation (N-term); Levuglandinyl - lysine hydroxylactam adduct	Phosphoglycerate kinase OS=Saccharomyces cerevisiae (strain ATCC 204508 / S288c) OX=559292 GN=PGK1 PE=1 SV=2
P06169|PDC1_YEAST	243.1	9	9	Carbamidomethylation	Pyruvate decarboxylase isozyme 1 OS=Saccharomyces cerevisiae (strain ATCC 204508 / S288c) OX=559292 GN=PDC1 PE=1 SV=7
P00924|ENO1_YEAST	228.77	13	5	Phenethyl isothiocyanate	Enolase 1 OS=Saccharomyces cerevisiae (strain ATCC 204508 / S288c) OX=559292 GN=ENO1 PE=1 SV=3
P10591|HSP71_YEAST	222.5	7	1	Carbamidomethylation	Heat shock protein SSA1 OS=Saccharomyces cerevisiae (strain ATCC 204508 / S288c) OX=559292 GN=SSA1 PE=1 SV=4
P00950|PMG1_YEAST	210.63	10	10		Phosphoglycerate mutase 1 OS=Saccharomyces cerevisiae (strain ATCC 204508 / S288c) OX=559292 GN=GPM1 PE=1 SV=3
P32324|EF2_YEAST	204.75	9	9		Elongation factor 2 OS=Saccharomyces cerevisiae (strain ATCC 204508 / S288c) OX=559292 GN=EFT1 PE=1 SV=1
P10592|HSP72_YEAST	173.7	6	0	Carbamidomethylation	Heat shock protein SSA2 OS=Saccharomyces cerevisiae (strain ATCC 204508 / S288c) OX=559292 GN=SSA2 PE=1 SV=3
P14540|ALF_YEAST	171.85	7	7	Carbamidomethylation	Fructose-bisphosphate aldolase OS=Saccharomyces cerevisiae (strain ATCC 204508 / S288c) OX=559292 GN=FBA1 PE=1 SV=3
P00549|KPYK1_YEAST	166.49	6	6	Carbamidomethylation; Monoglutamyl	Pyruvate kinase 1 OS=Saccharomyces cerevisiae (strain ATCC 204508 / S288c) OX=559292 GN=CDC19 PE=1 SV=2
P22202|HSP74_YEAST	162.29	5	1	Carbamidomethylation; Acetylation (N-term); Methyl ester	Heat shock protein SSA4 OS=Saccharomyces cerevisiae (strain ATCC 204508 / S288c) OX=559292 GN=SSA4 PE=1 SV=3
P14832|CYPH_YEAST	147.4	5	4	Carbamidomethylation; Acetylation (N-term)	Peptidyl-prolyl cis-trans isomerase OS=Saccharomyces cerevisiae (strain ATCC 204508 / S288c) OX=559292 GN=CPR1 PE=1 SV=3
P09435|HSP73_YEAST	133.64	3	1	Carbamidomethylation; Acetylation (K); Methyl ester	Heat shock protein SSA3 OS=Saccharomyces cerevisiae (strain ATCC 204508 / S288c) OX=559292 GN=SSA3 PE=1 SV=3
P12709|G6PI_YEAST	115.48	5	5	Acetylation (N-term); Dehydration; Carbamidomethylation (DHKE X@N-term)	**Glucose-6-phosphate isomerase** OS=Saccharomyces cerevisiae (strain ATCC 204508 / S288c) OX=559292 GN=**PGI1** PE=1 SV=3
P10081|IF4A_YEAST	112.47	4	4	Phosphorylation (STY); Carbamylation; Carbamidomethylation (DHKE X@N-term)	ATP-dependent RNA helicase eIF4A OS=Saccharomyces cerevisiae (strain ATCC 204508 / S288c) OX=559292 GN=TIF1 PE=1 SV=3
P16474|BIP_YEAST	102.36	3	1	Methyl ester	Endoplasmic reticulum chaperone BiP OS=Saccharomyces cerevisiae (strain ATCC 204508 / S288c) OX=559292 GN=KAR2 PE=1 SV=1
P00445|SODC_YEAST	99.37	2	2	Carbamidomethylation	Superoxide dismutase [Cu-Zn] OS=Saccharomyces cerevisiae (strain ATCC 204508 / S288c) OX=559292 GN=SOD1 PE=1 SV=2
P00942|TPIS_YEAST	96.54	2	2	Carbamidomethylation (DHKE X@N-term)	Triosephosphate isomerase OS=Saccharomyces cerevisiae (strain ATCC 204508 / S288c) OX=559292 GN=TPI1 PE=1 SV=2
P29311|BMH1_YEAST	89.87	2	1	Acetylation (N-term)	Protein BMH1 OS=Saccharomyces cerevisiae (strain ATCC 204508 / S288c) OX=559292 GN=BMH1 PE=1 SV=4
P34730|BMH2_YEAST	87.2	2	1	Acetylation (N-term)	Protein BMH2 OS=Saccharomyces cerevisiae (strain ATCC 204508 / S288c) OX=559292 GN=BMH2 PE=1 SV=3
P23254|TKT1_YEAST	78.91	2	2		Transketolase 1 OS=Saccharomyces cerevisiae (strain ATCC 204508 / S288c) OX=559292 GN=TKL1 PE=1 SV=4
P20081|FKBP_YEAST	56.74	2	2	Acetylation (N-term)	FK506-binding protein 1 OS=Saccharomyces cerevisiae (strain ATCC 204508 / S288c) OX=559292 GN=FPR1 PE=1 SV=2

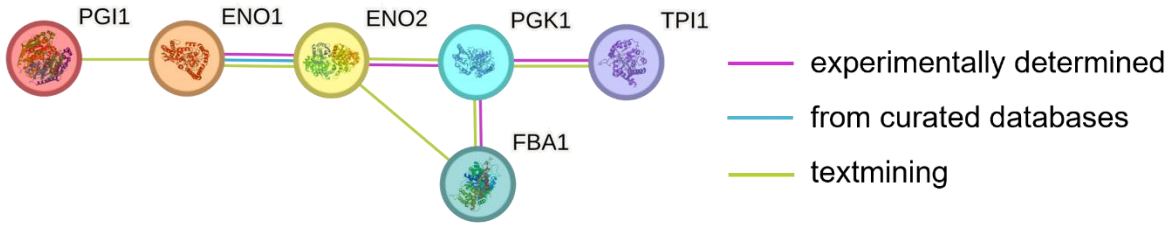

***Fig. 9**: STRING database network of PGI1 and interaction partners. PGI1 and its interaction partners were identified via LC-MS in the elution of a µNANEX purification of 20 µL yeast lysate expressing PGI1-GFP. A connection between two protein nodes indicates that previous studies have provided evidence of a physical interaction between these proteins with medium confidence.*

9. Recoveries for different trapper affinities

***Table 4**: Recoveries predicted by the µNANEX digital twin model for different trappers with different affinities for the analyte. Reference conditions were implemented with for the stripper a k_{on} of 5 10^5 M^{-1} s^{-1} and for the trapper a k_{on} of 3 10^5 M^{-1} s^{-1}.*

k_{off} trapper (s^{-1})	K_D k_{off}/k_{on}	Recovery (%)
3	10 µM	0
1.2	4 µM	12
6 10^{-1}	2 µM	55
3 10^{-1}	1 µM	96
1.2 10^{-1}	400 nM	100
6 10^{-2}	200 nM	96
3 10^{-2}	100 nM	81
3 10^{-3}	10 nM	19
3 10^{-4}	1 nM	2

10. References

1 R. Hansen, H. Bruus, T. H. Callisen and O. Hassager, *Langmuir*, 2012, **28**, 7557–7563.

2 Coulson and Richardson, *Flow of fluids through granular beds and packed columns*, 1991.

3 C. Song, P. Wang and H. A. Makse, *Nature*, 2008, **453**, 629–632.

4 G. Desmet and K. Broeckhoven, *Anal Chem*, 2008, **80**, 8076–8088.

5 S. Deridder and G. Desmet, *J Chromatogr A*, 2012, **1227**, 194–202.

6 Y. Yao and A. M. Lenhoff, *J Chromatogr A*, 2006, **1126**, 107–119.

7 D. Ruthven, *Principles of adsorption and adsorption processes*, 1984.

8 S. Datta and S. Ghosal, *Lab Chip*, 2009, **9**, 2537–2550.

9 J. L. Dores-Sousa, J. De Vos and S. Eeltink, *J Sep Sci*, 2019, **42**, 38–50.

10 J. M. P. Q. Delgado, *Heat and Mass Transfer/Waerme- und Stoffuebertragung*, 2006, **42**, 279–310.

11 Y. Huang and J. H. Seinfeld, *Atmos Environ X*, DOI:10.1016/J.AEAOA.2019.100006.

12 A. Ogata and R. B. Banks, *Geological survey professional paper*, DOI:https://doi.org/10.3133/pp411A.

13 F. Hagemann, P. Adametz, M. Wessling and V. Thom, *J Chromatogr A*, , DOI:10.1016/j.chroma.2020.461319.

14 M. C. Nweke, R. G. McCartney and D. G. Bracewell, *J Chromatogr A*, 2017, **1530**, 129–137.

15 M. Djabourov, A. H. Clark, D. W. Rowlands and S. B. Ross-Murphy, *Macromolecules*, 2002, **22**, 180–188.

16 GraphPad Prism 9 Curve Fitting Guide - Equation: One phase decay, https://www.graphpad.com/guides/prism/latest/curve-fitting/reg_exponential_decay_1phase.htm, (accessed 19 June 2023).

17 GraphPad Prism 9 Curve Fitting Guide - Equation: Association kinetics (two ligand concentrations) , https://www.graphpad.com/guides/prism/latest/curve-fitting/reg_association2.htm, (accessed 19 June 2023).

18 stdshade - File Exchange - MATLAB Central, https://nl.mathworks.com/matlabcentral/fileexchange/29534-stdshade, (accessed 31 July 2024).